J Intell Manuf (2008) 19:473–483
DOI 10.1007/s10845-008-0097-1

Estimation of cutting forces and surface roughness for hard turning using neural networks

Vishal S. Sharma · Suresh Dhiman · Rakesh Sehgal · S. K. Sharma

Received: 8 September 2007 / Accepted: 12 February 2008 / Published online: 14 March 2008

Abstract Metal cutting mechanics is quite complicated and it is very difficult to develop a comprehensive model which involves all cutting parameters affecting machining variables. In this study, machining variables such as cutting forces and surface roughness are measured during turning at different cutting parameters such as approaching angle, speed, feed and depth of cut. The data obtained by experimentation is analyzed and used to construct model using neural networks. The model obtained is then tested with the experimental data and results are indicated.

Keywords Cutting forces · Surface roughness · Neural networks

Introduction

The basic operation of turning is one of the most commonly employed operations in experimental work of metal cutting. The work material is held in the chuck of a lathe and rotated. The tool is held rigidly in a tool post and moved at a constant rate along the axis of the bar (feed), cutting away a layer of metal to form a profile. The forces acting on the tool are an important aspect of machining. Knowledge of the cutting forces is needed for estimation of power requirements and for the design of machine tool elements, tool-holders and fixtures, adequately rigid and free from vibration. Many force measurement devices like dynamometers have been developed which are capable of measuring tool forces with increasing accuracy. Power consumed in metal cutting is largely converted into heat near the cutting edge of tool, and many of the economic and technical problems of machining are caused directly or indirectly by this heating action. The cost of machining is strongly dependent on the rate of material removal, and costs may be reduced by increasing the cutting speed and/or the feed rate, there are limits to the speed and feed above which the life of the tool is shortened excessively. Another important cutting variable in machining is surface roughness. The need for the products with very fine surface finish keeps increasing rapidly because of new application in various fields like aerospace, automobile, die and mold manufacturing. Machined surface characteristics are important in determining the functional performance such as fatigue strength, corrosion resistance and tribological properties of machined components. The quality of surfaces of machined components is determined by the surface finish and integrity obtained after machining. High surface roughness values, hence poor surface finish, decrease the fatigue life of machined components. It is therefore clear that control of the machined surface is essential.

The equation for modeling surface roughness is:

$$R_a = \frac{f^2}{32 r_e}. \quad (1)$$

where R_a: surface roughness (mm), f: feed rate (mm/rev), r_e: tool nose radius (mm).

According to this model, to decrease the feed rate or increase the tool nose radius to improve surface finish. The problem with this model is that it does not take into account

V. S. Sharma (✉)
Department of Industrial Engineering, National Institute of Technology, Jalandhar, Punjab, India
e-mail: sharmavs@nitj.ac.in; vishal_sim@yahoo.com

S. Dhiman · R. Sehgal
Department of Mechanical Engineering, National Institute of Technology, Hamirpur, Himachal Pradesh, India

S. K. Sharma
Department of Mechanical Engineering, National Institute of Technology, Kurukshetra, Hariyana, India

any imperfections in the process—such as tool vibration or chip adhesion.

The current study takes into account cutting forces and surface roughness for analysis and modeling.

The work of other researchers is indicated below.

Rahman et al. (1995) presented a neural-network-based approach for on-line fault diagnosis scheme which monitors the level of tool wear, chatter vibration and chip breaking in a turning operation. The experimental results showed that the neural network has a high prediction success rate.

Thiele and Melkote (1999) determined the effects of workpiece hardness and tool edge geometry on surface roughness in finish hard turning using CBN tools. They conducted an analysis of variance (ANOVA), after completing the experiments, to discern whether differences in surface quality between various runs were statistically significant. This analysis found that edge geometry and feed rate impacted surface quality. In addition, the ANOVA showed that the interaction between the hardness and edge geometry, and the interaction between hardness and feed rate were significant.

Dimla (1999) investigated study into the application of perceptron type neural networks to tool state classification during metal turning operation.

Liang et al. (2000) presented an integrated approach to simultaneous optimization of machining parameters, including machining speed, feed rate and depth of cut, number of passes, tool adjustment interval, and the amount of adjustment and found that tool adjustment interval and amount of adjustment depend not only on the amount of material being removed, but also on the cutting speed, feed and depth of cut.

Feng and Wang (2002) developed an empirical model using non linear regression analysis with logarithmic data transformation during turning of steel (8620) HRB86 with carbide inserts having multiphase coatings. They studied impact of work piece hardness, feed, tool point angle, Depth of cut, spindle speed and cutting time on the surface roughness. The values of surface roughness predicted by the model were then verified with the experiments and observed that model produced smaller error.

Srinivasa et al. (2002) presented an estimation of flank wear in face milling operations using radial basis function (RBF) networks. Various signals such as acoustic emission (AE), surface roughness, and cutting conditions (cutting speed and feed) were used to estimate the flank wear. The hidden layer RBF units were fixed randomly from the input data and using batch fuzzy C means algorithm, and a comparative study was carried out. They compared results obtained from a fixed RBF network with those from a resource allocation network (RAN).

Chou et al. (2002) utilized a similar approach to determine the impact of various parameters to surface roughness and flank wear in finish hard turning of hardened steel with CBN tools. They reduced the number of factors to three—cutting speed, CBN content percentage, and length of the cuts. They only tried to understand the factors important in finish hard turning with CBN tools.

Zuperl and Cus (2003) presented a neural network-based approach to complex optimization of cutting parameters. They described the multi-objective technique of optimization of cutting conditions by means of the neural networks taking into consideration the technological, economic and organizational limitations.

Özel and Karpat (2005) utilized neural network modeling to predict surface roughness and tool flank wear over the machining time for variety of cutting conditions in finish hard turning.

Haci et al. (2006) performed the comparison of measured and calculated results of cutting force components and temperature variation generated on the tool tip in turning for different cutting parameters and different tools having various tool geometries while machining AISI 1040 steel, hardened at HRc 40. Finally, they analyzed effects of cutting parameters and tool geometry on cutting forces and tool tip temperature. The average deviation between measured and calculated force results were found as 0.37%.

Sharma et al. (2006) developed model using adaptive neuro fuzzy inference system for predicting tool wear using cutting forces, vibrations and acoustic emissions. They could establish close relation between the predicted and the actual tool wear values.

Feng et al. (2006) proposed a procedure for selection and cross-validation of predictive regression analysis and neural network models. Experimental data from turning surface roughness study was used to demonstrate the proposed concept.

Alajmi and Alfares (2007) presented a model used for prediction of cutting forces. In this study cutting forces prediction was modeled using back propagation (BP) neural network with an enhancement by differential evolution (DE) algorithm. Experimental machining data was used in this study to train and evaluate the model. The data included speed, feed rate, depth of cut, nose wear, flank wear, notch wear, feed force, vertical force, and radial force. The results showed an improvement in the reliability of predicting the cutting forces over the previous work.

Singh and Rao (2007) conducted experimental investigation to determine the effects of cutting conditions and tool geometry on the surface roughness in the finish hard turning of the bearing steel (AISI 52100). Mixed ceramic inserts made up of aluminium oxide and titanium carbonitride (SNGA), having different nose radius and different effective rake angles, were used as the cutting tools.

The literature reveals that not much work is reported on estimation of cutting forces and surface roughness for hard turning using neural networks. So the objective of this study is to analyze the effect cutting parameters on machining

variables and formulate model for estimation cutting forces and surface roughness using neural networks.

Experimental set up and procedure

The material Adamite is used for investigation. This material is chosen based on its wide applications as die and mould, roller and ball bearings, manufacturing material for balls for shot peening/blasting/barrel cleaning etc. Chemical composition of Adamite was tested on Spark Emission Spectrometer (Make Baird, USA) and the same is given in Table 5 (Appendix III). Hardness of the specimen was tested on micro-hardness tester (Make Akashi MVKH2) and given in Table 5 (Appendix III). The machining experiments were carried out on all geared high precision (Digital Read Out) Lathe, by using indexable coated carbide insert (CCMT090304). The inserts with multilayer chemical vapour deposition (CVD) coating and cobalt enriched substrate has been used. CVD coating consists of thick medium-temperature chemical vapour deposition (MTCVD) TiCN (4 μm) for wear resistance and thermally stable Al_2O_3 (8 μm) for crater resistance. The combination of the top coating and the gradient substrate gives the extremely good behavior in dry machining. All the inserts used for the experiments had same geometry. The experiments were conducted to measure cutting force (F_c), passive force (F_p), feed force (F_f) and surface roughness (R_a) at different approaching angles, speed, feed and depth of cut. The variations of cutting parameters adopted for carrying out experimentation is given in Appendix I. In total 52 experiments were conducted and 30 were used to construct the model and investigate the effect

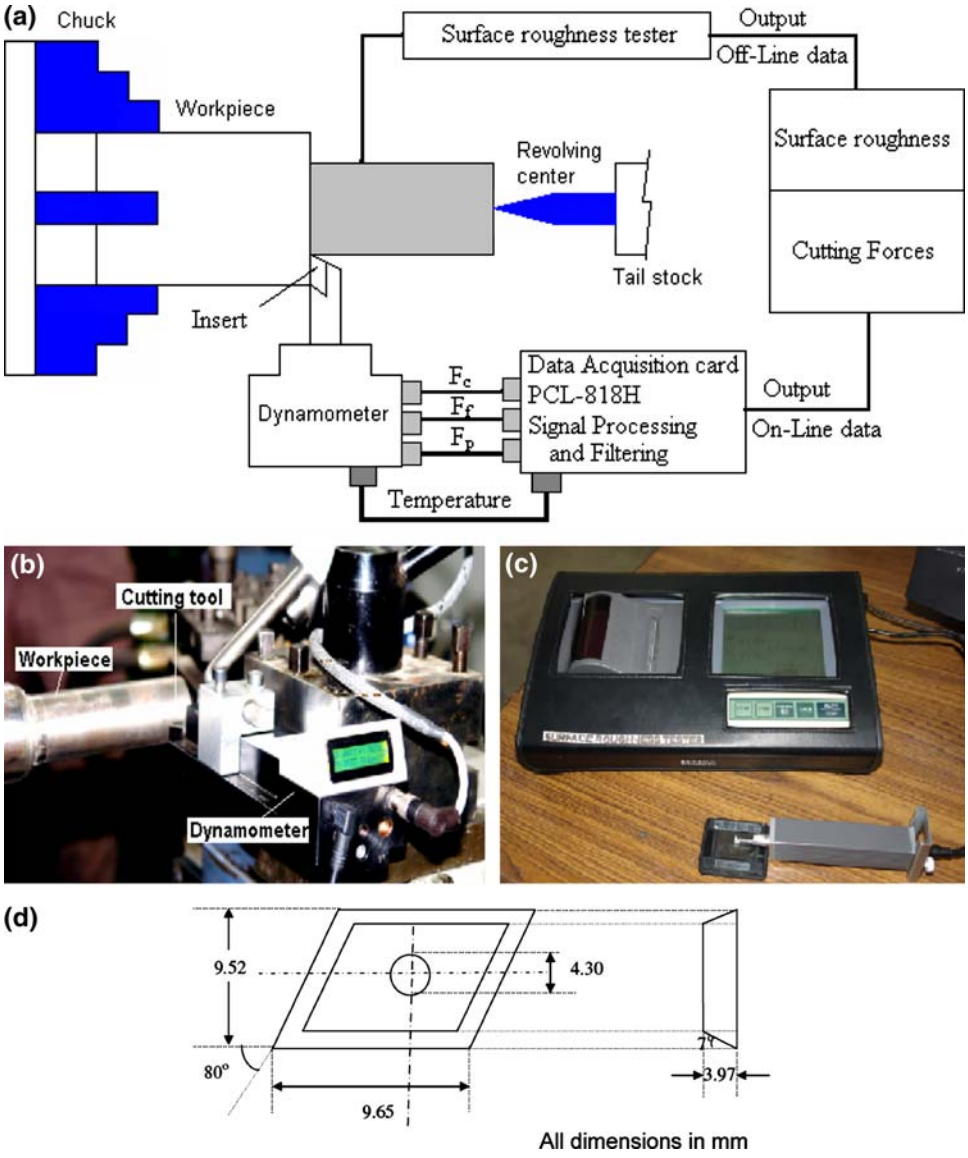

Fig. 1 Experimental setup. (**a**) Schematic layout of experimental setup, (**b**) photograph of experimental setup showing dynamometer, (**c**) photograph of surface roughness tester, (**d**) sketch of carbide insert used for machining

of cutting parameters on machining variables. The remaining experiments are used for model testing and validation. The turning operations were carried out for different cutting parameters as shown in the Table 5.

The schematic layout of the experimental setup is shown in Fig. 1a. A three component turning dynamometer (TeLC DKM 2010, Germany make) was used to measure cutting forces on all geared head high precision (DRO) Lathe. The longitudinal turning was conducted and the length of cut for each test was 25 mm. The turning dynamometer was rigidly held on the tool post so that cutting forces F_c, F_f, F_p) could be measured (refer Fig. 1b). Force signals obtained from the dynamometer were transferred to computer by means of the data acquisition card and then were evaluated by using XKM software. Figure 1d gives a sketch of the carbide insert used for experimentation. Surface roughness tester (SJ-301, Mitotoyo make-refer Fig. 1c) was used to measure surface roughness (R_a) after each turning operation.

Analysis and discussions

Analysis for cutting force (F_c)

Regression equation for cutting force (F_c) obtained from the experimental data (Set I-Appendix I) is given in Eq. 2. Figure 2 shows the effect of the all cutting parameters i.e. approaching angle, speed, feed and depth of cut on cutting force (F_c). The actual factors are A: approaching angle = 67.50, B: speed = 116.30, C: feed = 0.19, D: depth of cut = 0.90.

This graph indicates that as approaching angle, feed and depth of cut is increased, the cutting force (F_c) also increases. The speed has negative impact on cutting forces (F_c) i.e. as the speed increases the cutting forces (F_c) decreases. The depth of cut has maximum influence on the cutting force (F_c) followed by feed and the approaching angle. The increase in speed leads to high temperature and hence softening of the workpiece material and as a result the cutting force shows a decreasing trend. On other hand with the increase in feed, approaching angle and depth of cut, cutting force increases. The depth of cut influences the cutting force the most because as the depth of cut increases, the maximum cutting edge angle increases which leads to increase in cutting force component.

$$F_c = -77.89992 + 1.51196 \times A - 0.29639 \times B + 907.09759 \times C + 354.15297 \times D. \quad (2)$$

Analysis for passive force (F_p)

Regression equation for passive force (F_p) obtained from the experimental data (Set I-Appendix I) is given in Eq. 3.

$$F_p = +473.83835 - 2.92017 \times A + 0.60115 \times B + 285.55367 \times C + 202.10955 \times D. \quad (3)$$

Figure 3 shows the effect of various cutting parameters on passive force (F_p). It is observed that as any of the cutting variables i.e. speed, feed and depth of cut increases, passive force (F_p) also increases. Out of various cutting parameters depth of cut influences passive force (F_p) the most. F_p reduces as approaching angle increases.

Speed and feed have almost the same effect i.e. it increases F_p. The reason for depth of cut contributing more to passive force (F_p) is that with the increase in depth of cut tool chip interface area increases which leads to increase in passive force.

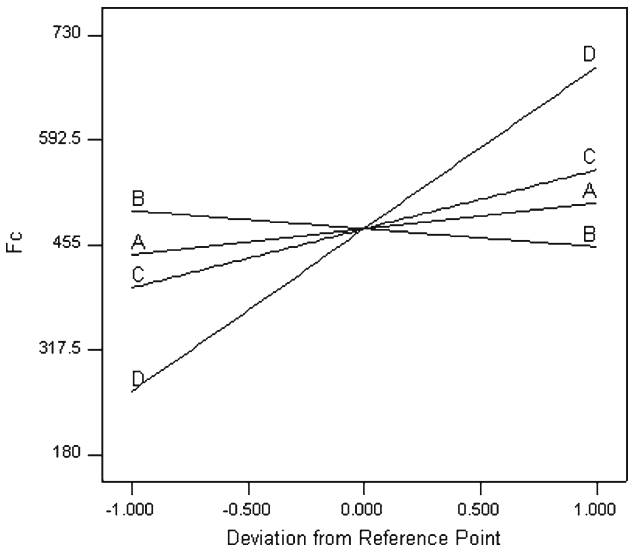

Fig. 2 Effect of cutting parameters on cutting force (F_c)

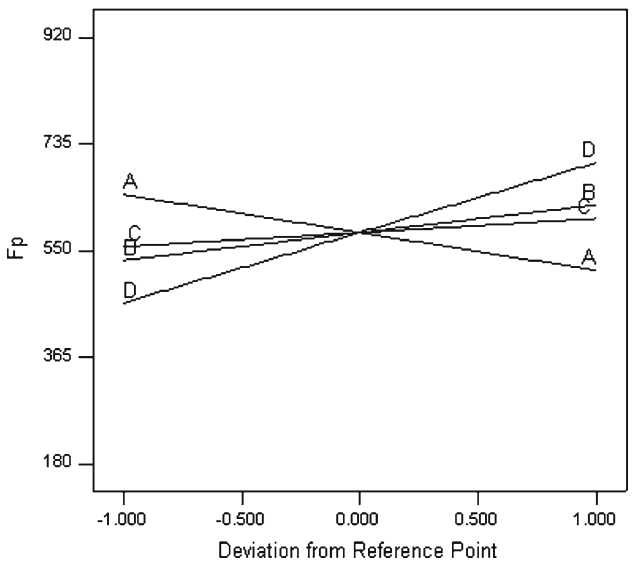

Fig. 3 Effect of cutting parameters on passive force (F_p)

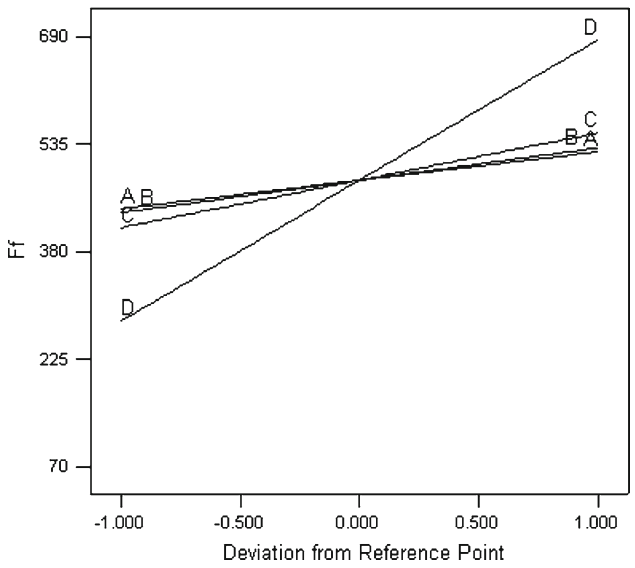

Fig. 4 Effect of cutting variables on feed force F_f

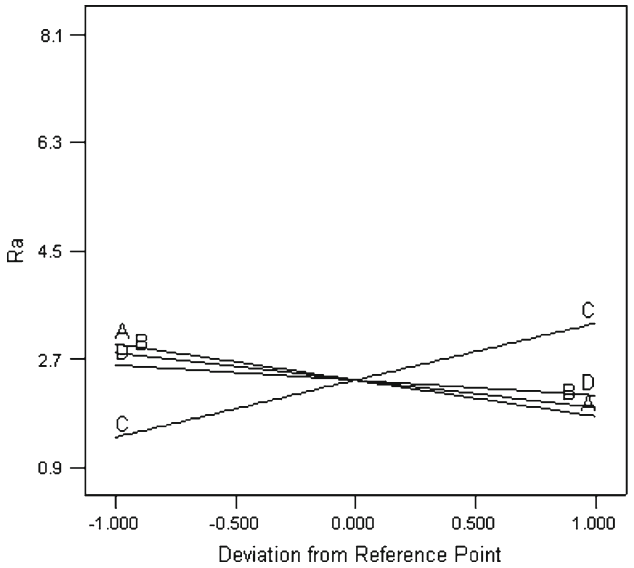

Fig. 5 Effect of cutting parameters on Surface roughness (R_a)

Analysis for feed force (F_f)

Regression equation for feed force (F_f) obtained from the experimental data (Set I-Appendix I) is given in Eq. 4. Figure 4 shows the effect of various cutting parameters on feed force (F_f). This graph clearly indicates that as approaching angle, speed, feed and depth of cut increases, feed force (F_f) also increases.

$$F_f = -160.80965 + 1.82092 \times A + 0.58641 \times B + 802.11825 \times C + 337.93308 \times D. \quad (4)$$

The depth of cut seems to influence feed force (F_f) component more significantly than the cutting speed, feed and approaching angle because with the increase in depth of cut, the maximum cutting edge angle increases.

Analysis for surface roughness (R_a)

Regression equation for surface roughness (R_a) obtained from the experimental data (Set I-Appendix I) is given in Eq. 5. Figure 5 shows the effect of various cutting parameters i.e approaching angle, speed, feed and depth of cut on surface roughness (R_a). It is evident that as feed increases surface roughness (R_a) also increases whereas approaching angle, speed and depth of cut have negative effect on surface roughness. By increasing the cutting speed the surface roughness decreases, because formation of built-up-edge (BUE) is favored in a certain range of cutting speed. By increasing cutting speed beyond this region, BUE will be eliminated and as a result surface finish will improve.

$$R_a = +3.14105 - 0.026776 \times A - 5.70638E - 003 \times B + 11.14522 \times C - 0.42052 \times D. \quad (5)$$

Also at low cutting speed, grooves develop on flank wear land which causes degradation of newly formed surface. But with increase in speed these grooves gradually reduce thus enhancing the surface finish. Even the lateral plastic flow of the workpiece material along the cutting edge direction may increase the peak to valley height of surface irregularities. With the increase in depth of cut, the surface roughness value increases, because with increase in depth of cut chatter may result causing degradation of the workpiece surface.

Artificial neural network model (ANN)

ANNs are very efficient on adaptation and learning and for this reason they are used as modelling tools in a number of applications. An ANN is made of three types of layers: an input layer which accepts the input variables, herein approaching angle, speed, feed and depth of cut. Hidden layers has some number of neurons, and an output layer made of four neuron that in the case examined herein gives the F_c, F_f , F_p and R_a (refer Fig. 6). Hidden and output layers are composed of some number of neurons that perform a specific nonlinear function such as sigmoid. The neurons of one layer are interconnected to the neurons of the pre and after layers through weighted links. Each neuron of the hidden and output layers is offset by a threshold value. The back-propagation training algorithm is used here which iteratively minimizes the cost function with respect to the interconnection weights and

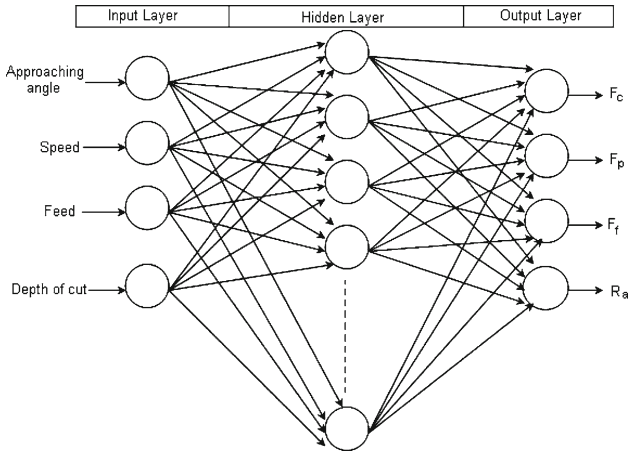

Fig. 6 Neural network architecture

neuron thresholds. The training process is terminated either when the mean square error (MSE) between the measured data points and the predicted ANN values for all elements in the training set has reached a pre-specified threshold or after the completion of a pre-selected number of learning iterative processes, called learning epochs Simpson (1992). The selection of number of neurons in the hidden layer and number of epochs is quite tricky task in deciding the structure of the ANN. Here they are obtained by optimization process. The whole data is divided into 3 sets. Set I is training data, Set II is testing data and Set III is validation data (Appendix I). The training data is trained with 10, 20, 30, 40 and 50 number of neurons along with 100, 200, 300, 400 and 500 epochs. The time taken for the training process is referred as training time. Training time and mean square error are noted for each combination neurons and epochs. After training each model is tested with the testing data and testing error (test error) is also noted for each combination (Table 6-Appendix III). The optimal structure of the neural network is found by minimizing test error with testing data, minimizing training time and mean square error for training data. The optimization problem is approximated by the following equations and then solved. The regression equations i.e Eqs. 7 and 8 for number of neurons and epochs are obtained from the data in Table 6 (Appendix III).

$$\text{Find} X = [\text{No. of neurons, No. of epochs}]. \tag{6}$$

$$\begin{aligned}\text{No. of neurons} = {} & 3.00116 - 0.065808 \times \text{Test error} \\ & + 0.53215 \times \text{Training time} \\ & + 214.10478 \times \text{Mean square error}.\end{aligned} \tag{7}$$

$$\begin{aligned}\text{No. of epochs} = {} & +909.12491 + 1.41876 \times \text{Test error} \\ & - 0.98830 \times \text{Training time} \\ & - 9379.77264 \times \text{Mean square error}.\end{aligned} \tag{8}$$

$$\begin{aligned}\text{to minimize} \quad & f(X) = \text{Test error}, \\ & f(X) = \text{Training time and} \\ & f(X) = \text{Mean square error}.\end{aligned} \tag{9}$$

$$\text{Subjected to} \quad \begin{aligned} & 10 \le \text{No. of neurons} \le 50 \\ & 100 \le \text{No. of epochs} \le 500 \end{aligned}. \tag{10}$$

The optimum values of cutting variables based on the maximum desirability are selected from row 1 of Table 7 (Appendix III). So the structure with one hidden layer with 20 neuron and 323 epochs is selected.

Figure 7a shows a graph indicating the effect of number of neurons on test error, training time and mean square error. It is quite clear here that training time is most prominent here and it increses as the number of neurons increase. Figure 7b shows a graph indicating the effect of number of epochs on test error, training time and mean square error. It is seen that mean square error is quite significant here and it decreases with the increase in number of epochs.

Model for cutting force (F_c)

Figure 8 shows the comparison between the actual experimental and estimated values of F_c obtained using neural network (Appendix II). Hidden line represents the actual values of F_c. The continuous dark line indicates the estimated values of F_c obtained using neural networks. It can be seen from the Fig. 8 that both estimated values are close to actual vales of F_c. Hence it is evident that there is good agreement between estimated and experimental values of F_c, which confirms the validity of the models. The average error for this model is 5.4%.

Model for passive force (F_p)

Figure 9 shows the comparison between estimated F_p obtained using neural network versus actual experimental F_p (Appendix II). Dark line represents the trend of F_p obtained by using neural network model, whereas, hidden line represents the trend of experimental F_p. It is seen that both lines are quite close to each other. The average error is for this model is 30%.

Model for feed force (F_f)

Referring Fig. 10 indicates the comparison between the estimated F_f obtained using neural networks versus actual experimental F_f (Appendix II). Continuous line represents the trend of F_f obtained by using neural network model, whereas, hidden line represents the trend of experimental F_f. It can be seen that both the lines are close to each other and

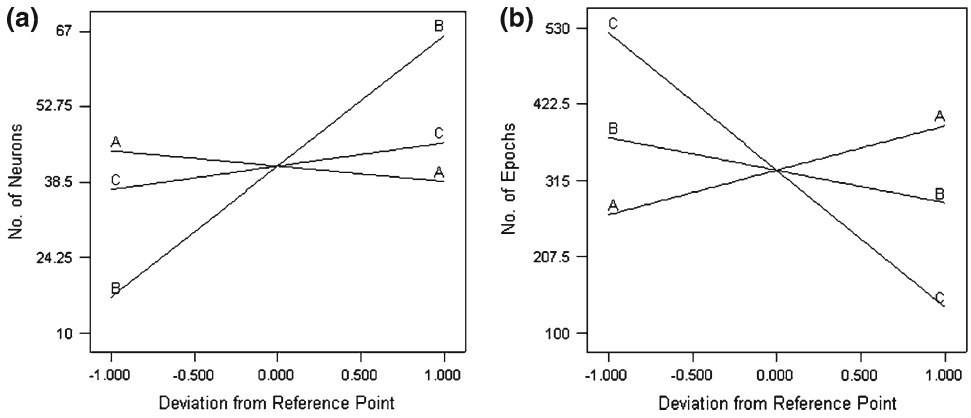

Fig. 7 Effect of number of neurons and epochs. Actual Factors: *A*: test error = 28.52; *B*: training time = 51.49; *C*: mean square error = 0.06

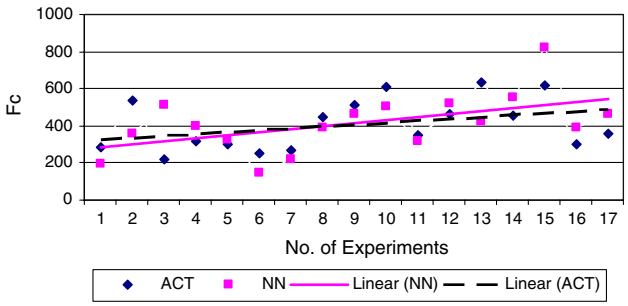

Fig. 8 Comparison of actual and estimated for F_c

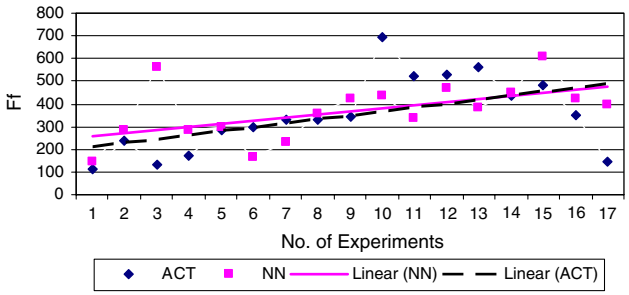

Fig. 10 Comparison of actual and estimated for F_f

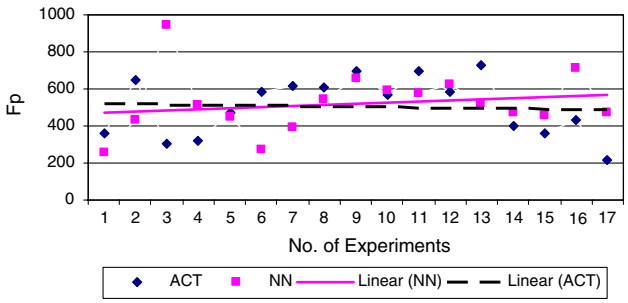

Fig. 9 Comparison of actual and estimated for F_p

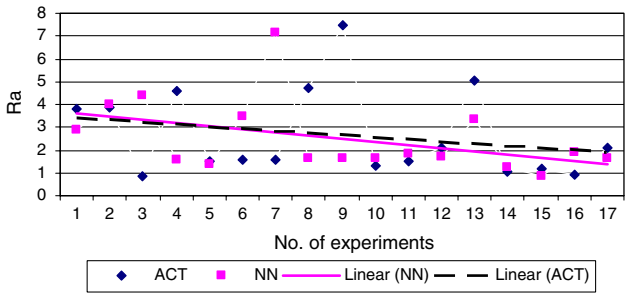

Fig. 11 Comparison of actual and estimated for R_a

at one place even cross each other. So this model can also predict with accuracy. The average error for this model is 16.5%.

Model for surface roughness (R_a)

Figure 11 shows the comparison between the behavior of estimated R_a obtained using neural network versus actual experimental R_a (Appendix II). Continuous line represents the trend of R_a obtained by using neural network model, whereas, hidden line represents the trend of experimental R_a. The average error for this model is 42.2

Conclusions

In this course of study, machining variables such as cutting forces and surface roughness are measured in turning of adamite. The effect of cutting parameters such as approaching angle, speed, feed and depth of cut on machining variables

are evaluated. The model is formulated for all cutting parameters and machining variables using neural networks. Then the models are compared for their prediction capability with the actual values. The model gave overall 76.4% accuracy.

The following conclusions can be made from the investigations.

1. Cutting force (F_c) shows an increasing trend with the increase in approaching angle, feed and depth of cut where as it shows a decreasing trend with speed. The neural network model for cutting force (F_c) could predict with high accuracy.
2. Passive force (F_p) increases with increase in depth of cut, speed and feed where as it shows decreasing trend with increase in approaching angle. The depth of cut exhibits maximum influence on passive force (F_p) as compared to the other cutting parameters. The neural network model for cutting force F_p could predict with moderate accuracy.
3. Feed force (F_f) shows increasing trend with all variables i.e approaching angle, speed, feed and depth of cut. The depth of cut exhibits maximum influence on the feed force (F_f). The neural network model for cutting force F_f could predict well.
4. Surface roughness (R_a) is positively influenced with feed and it shows negative trend with approaching angle, speed and depth of cut. The neural network model for cutting force R_a could predict with moderate accuracy.

Approaching angle influences cutting force (F_c,) feed force (F_f) positively, passive force (F_p) and surface roughness (R_a) negativley. Speed influences passive force (F_p) and feed force (F_f) positively, cutting force (F_c) and surface roughness (R_a) negatively. Feed influences cutting force (F_c), feed force (F_f), passive force (F_p), surface roughness (R_a) positively. Depth of cut influences cutting force (F_c), passive force (F_p), feed force (F_f) positively and surface roughness (R_a) negatively.

Appendix I: Experimental data

Table 1 Set I: Training data

Ex	Approaching angle	Speed	Feed	DOC	Cutting forces			Surface roughness R_a
					F_c	F_f	F_p	
1	45	36.6	0.1	0.3	186	73	263	2.8
2	45	36.6	0.1	0.9	395	163	459	3.88
3	45	36.6	0.1	1.5	687	549	914	3.92
4	45	81.7	0.1	0.6	247	229	529	1.34
5	45	196	0.1	0.6	209	210	462	1.25
6	45	36.6	0.17	0.6	255	145	263	3.33
7	45	36.6	0.27	0.6	380	179	360	6.98
8	60	36.6	0.1	0.3	222	237	560	1.47
9	60	36.6	0.1	0.9	453	479	668	1.44
10	60	36.6	0.1	1.5	626	549	634	1.59
11	60	51.5	0.1	0.6	282	298	556	1.54
12	60	196	0.1	0.6	277	397	670	1.61
13	60	36.6	0.17	0.6	387	309	552	3.25
14	60	36.6	0.27	0.3	256	291	561	1.43
15	60	36.6	0.27	0.9	515	648	579	1.48
16	60	36.6	0.27	1.5	690	690	621	1.53
17	75	36.6	0.1	0.6	373	452	529	1.67
18	75	51.5	0.1	0.6	357	480	591	1.48
19	75	81.7	0.1	0.6	352	495	629	1.61
20	75	196	0.1	0.6	341	498	664	1.28
21	75	36.6	0.17	0.6	557	554	652	3.52
22	75	36.6	0.27	0.6	729	578	801	8.04
23	90	36.6	0.1	0.3	231	212	391	1.25
24	90	36.6	0.1	0.6	367	377	408	1.16
25	90	36.6	0.1	1.2	526	461	380	1.1
26	90	51.5	0.1	0.6	241	148	247	1.24
27	90	81.7	0.1	0.6	265	166	206	1.02
28	90	126.6	0.1	0.6	273	235	271	0.98
29	90	36.6	0.13	0.6	249	112	180	1.51
30	90	36.6	0.21	0.6	502	202	257	2.82

Approaching angle, degrees; speed, m/min; feed, mm/rev; depth of cut (DOC), mm
F_c, F_f, F_p (cutting forces), Newtons; SR: R_a (surface roughness), μm

Table 2 Set II: Testing data

Ex	Approaching angle	Speed	Feed	DOC	Cutting forces			Surface roughness R_a
					F_c	F_f	F_p	
1	45	51.5	0.1	0.6	236	207	402	1.4
2	45	36.6	0.13	0.6	231	127	231	1.93
3	60	36.6	0.1	1.2	534	515	654	1.49
4	60	36.6	0.13	0.6	323	287	484	1.93

Approaching angle, degrees; speed, m/min; feed, mm/rev; depth of cut (DOC), mm
F_c, F_f, F_p (cutting forces), Newtons; SR: R_a (surface roughness), μm

Table 3 Set III: Validation data

Ex	Approaching angle	Speed	Feed	DOC	Cutting forces			Surface roughness R_a
					F_c	F_f	F_p	
1	45	36.6	0.1	0.6	281	110	357	3.82
2	45	36.6	0.1	1.2	540	237	647	3.9
3	45	126.6	0.1	0.6	219	130	306	0.84
4	45	36.6	0.21	0.6	319	175	319	4.57
5	60	36.6	0.1	0.6	302	282	470	1.53
6	60	81.7	0.1	0.6	256	297	587	1.56
7	60	126.6	0.1	0.6	270	330	616	1.6
8	60	36.6	0.21	0.6	444	330	610	4.73
9	60	36.6	0.27	0.6	511	341	693	7.49
10	60	36.6	0.27	1.2	613	695	572	1.28
11	75	126.6	0.1	0.6	347	524	700	1.5
12	75	36.6	0.13	0.6	462	527	584	2.07
13	75	36.6	0.21	0.6	631	561	729	5.04
14	90	36.6	0.1	0.9	455	437	404	1.07
15	90	36.6	0.1	1.5	614	484	357	1.16
16	90	196	0.1	0.6	298	350	430	0.94
17	90	36.6	0.17	0.6	357	148	219	2.12

Appendix II

Table 4 Estimated cutting forces (F_c, F_f, F_p) and surface roughenss (R_a)

	F_c	F_f	F_p	R_a
1	198.9679	145.9586	253.113	2.9174
2	361.12	282.5305	432.4871	4.0082
3	515.3155	559.1654	941.8641	4.3903
4	400.9554	287.1431	508.8088	1.5863
5	327.8533	297.924	447.2232	1.3837
6	149.9394	162.0836	270.6326	3.4627
7	216.7609	234.6429	391.3421	7.1724
8	389.7181	356.5466	545.7154	1.6501
9	460.4044	422.4928	653.0371	1.6654
10	504.6802	438.9434	588.0922	1.6501
11	313.6591	340.0809	572.7221	1.8254
12	522.7788	467.9554	625.144	1.6753
13	422.6182	381.8989	519.0946	3.3217
14	553.4023	450.5182	470.003	1.2352
15	823.5631	608.0617	458.4203	0.8702
16	388.4327	421.5863	711.0629	1.8857
17	460.4622	395.4795	471.3874	1.615

Appendix III

Table 5 Experimental design

Workpiece material	Adamite C = 1.85%; Si = 0.65%; Mn = 0.75%; P = 0.048%; S = 0.035%; Cr = 1.60%; Ni = 1.2%; Mo = 0.3	46.1 HRc
Tool material	Coated carbide insert	CCMT090304
Approaching angle (°)	45, 60, 75, 90	
Speed (m/min)	36.6, 51.5, 81.7, 19.6	
Feed rate (mm/rev)	0.1, 0.13, 0.17, 0.27	
Depth of cut (mm)	0.3, 0.6, 0.9, 1.5	
Rake angle (°)	6	

Table 6 Test error, test time and mean square error for different neurons and epochs

Test error	Test time	Mean square error	No. of neurons	No. of epochs
34	6.449	0.080045	10	100
39.554	6.068	0.077145	10	200
39.554	5.999	0.077145	10	300
39.5544	6.269	0.077145	10	400
34.28	5.048	0.077105	10	500
48.49	6.536	0.081346	20	100
29.426	10.045	0.069903	20	200
39.066	13.981	0.06879	20	300
38.9851	17.355	0.068138	20	400
36.1401	22.002	0.064085	20	500
72.318	9.483	0.080885	30	100
38.4017	17.485	0.07714	30	200
39.867	23.283	0.071757	30	300
41.2211	31.285	0.069209	30	400
41.3471	37.734	0.068731	30	500
33.34	14.2	0.076241	40	100
28.372	25.677	0.062642	40	200
−15.6	37.224	0.059206	40	300
35.392	49.391	0.054142	40	400
72.646	63.642	0.053994	40	500
43.175	21.762	0.074612	50	100
10.3791	38.386	0.059199	50	200
33.518	59.245	0.050823	50	300
41.157	74.818	0.045888	50	400
3.0711	97.93	0.040076	50	500

Table 7 Optimized results

Number	Test error	Training time	Mean square error	No. of neurons	No. of epochs	Desirability
1	−15.5999	5.048035	0.059612	19.47719	322.8596	0.708055
2	−15.5996	5.048086	0.059407	19.43344	324.7774	0.708041
3	−15.597	5.048269	0.059765	19.50999	321.4239	0.708037
4	−15.5936	5.048027	0.059041	19.35457	328.2224	0.70793
5	−15.4688	5.048409	0.058802	19.2954	330.6402	0.707504

References

Alajmi, M. S., & Alfares, F. (2007). Prediction of cutting forces in turning process using De-Neural Networks. *Artificial Intelligence and Applications, AIA 2007*, 2/12/2007–2/14/2007, Innsbruck, Austria.

Chou, Y. K., Evans, C. J., & Barash, M. M. (2002). Experimental investigation on CBN turning of hardened AISI 52100 steel. *Journal of Materials Processing Technology, 124*, 274–283.

Dimla, D. E. Sr. (1999). Application of perceptron neural networks to tool state classification in a metal turning operation. *Engineering Applications of Artificial Intelligence, 12*, 471–477.

Feng, C. X., & Wang, X. (2002). Development of empirical models for surface roughness prediction in finish turning. *International Journal of Manufacturing Technology, 20*, 348–356.

Feng, C.-X. J., Yu, Z.-G.(Samuel), & Kusiak, A. (2006). Selection and validation of predictive regression and neural network model based on designed experiments. *IIE Transactions, 38*, 13–23.

Haci, S., Faruk, U., & Yaldiz, S. (2006). Investigation of the effect of rake angle and approaching angle on main cutting force and tool tip temperature. *International Journal of Machine Tools & Manufacture, 46*(2), 132–141.

Liang, M., Mgwatu, M., & Zuo, M. (2000). Integration of cutting parameter selection and tool adjustment decisions for multipass turning. *International Journal of Advanced Manufacturing Technology, 17*(12), 861–869.

Özel, T., & Karpat, Y. (2005). Predictive modeling of surface roughness and tool wear in hard turning using regression and neural networks. *International Journal of Machine Tools and Manufacture, 45*(4–5), 467–479.

Rahman, M., Zhou, Q., & Hong, G. S. (1995). On-line cutting state recognition in turning using a neural network. *The International Journal of Advanced Manufacturing Technology, 10*(2), 87–92.

Sharma, V. S., Sharma, S. K., & Sharma, A. K. (2006). Tool wear estimation for turning operations. *Journal of Mechanical Engineering, 57*(3), 141–168.

Simpson, P. K. (1992). *Foundations of neural networks, artificial neural networks*. IEEE press.

Singh, D., & Rao, P. A. (2007). Surface roughness prediction model for hard turning process. *The International Journal of Advanced Manufacturing Technology, 32*(11–12), 1115–1124.

Srinivasa Pai, P., Nagabhushana, T. N., & Ramakrishna Rao, P. K. (2002). Flank wear estimation in face milling based on radial basis function neural networks. *International Journal Advanced Manufacturing Technology, 20*(4), 241–247.

Thiele, J. D., & Melkote, S. N. (1999). Effect of cutting edge geometry and workpiece hardness on surface generation in the finish hard turning of AISI 52100 steel. *Journal of Materials Processing Technology, 94*, 216–226.

Zuperl, U., & Cus, F. (2003). Optimization of cutting conditions during cutting by using neural networks. *Robotics and Computer Integrated Manufacturing, 19*, 189–199.